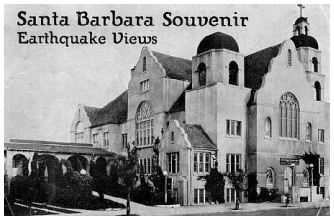

4th IASPEI / IAEE International Symposium:

Effects of Surface Geology on Seismic Motion

August 23–26, 2011 · University of California Santa Barbara

SEISMIC VERTICAL ARRAY ANALYSIS: PHASE DECOMPOSITION FOR S AND SURFACE WAVES

Kunikazu Yoshida
Geo-Research Institute
Itachibori 4-3-2, Nishi-ku,
Osaka 550-0012
JAPAN

ABSTRACT

It is important for interpretation of the seismic responses of a sedimentary basin to distinguish S and surface waves on strong-motion seismograms. A vertical array analysis method that decomposes S and surface waves from a set of surface and borehole seismic records (horizontal components) is proposed. Each of horizontal components of the array records assumed to consist of S wave and only one kind of surface (Love or Rayleigh) wave. The Fourier transform of each phase at the borehole is expressed as the product of the Fourier transform of that phase at the surface and the transfer function of that phase. I apply this method to a record of nearby intermediate-depth earthquake observed at a vertical array in the Ishikari plain, Japan. The array analysis result for ground motion show short duration of the direct S wave and late arrival surface waves with long duration. The estimated records are in good agreement with synthetic seismograms calculated by a 2-D finite difference method for a sedimentary basin model assuming vertical incident plain SH and SV waves. The simulation indicates that the basin-induced surface waves are generated at the southwestern basin edge and arrive at the array in the expected times.

INTRODUCTION

Observational seismic records from a sedimentary basin, such as the Ishikari plain, have large amplitude and long duration later phases compared with those obtained from an outside of the basin. Sometimes, these later phases contribute to severe damage in a sedimentary basin, as illustrated by various recent earthquakes such as the 1999 Izmit earthquake (Ozel and Sasatani, 2004), the 1999 Chi-chi earthquake (Fletcher and Wen, 2005), and the 2003 Tokachi-oki earthquake (Koketsu et al., 2005; Yoshida and Sasatani, 2005). Such two-dimensional or three-dimensional basin structural effects on wave propagation have been illustrated through observational (Uetake and Kudo, 1998, etc.) and numerical studies (Graves, 1993; Hisada et al., 1993; Kawase, 1996; Olsen and Archuleta, 1996, etc.).

Several seismic stations have been operated in the northwestern part of the Ishikari plain (Sasatani et al., 2001; Yoshida, 2004). The Ishikari plain has very thick (maximum thickness of sediments > 3 km) sedimentary basin structure. Seismic records derived from these seismic stations indicate significant effects of the sedimentary basin structure of large amplitude and long duration compared with those derived from outside of the basin (e.g. Yoshida and Sasatani, 2005).

It is important for interpretation of seismic responses of a sedimentary basin to distinguish S and surface waves on strong-motion seismograms. Yoshida and Sasatani (2006) and Yoshida and Sasatani (2008) have proposed a vertical array analysis method for phase decomposition from vertical array seismograms. However, this method is applicable to vertical array data that consists of seismic records obtained at more than 3 different depths. Although 7 borehole seismometer stations have operated in the Ishikari plain, these vertical array stations consist of surface and borehole seismometers. This decomposition method is not applicable for the vertical array data obtained from the stations in the Ishikari plain.

In the present study, a vertical array analysis method that decomposes S and surface waves from a set of surface and borehole seismic

records (horizontal components) is proposed. This method is applied for vertical array data observed at the northwestern part of the Ishikari plain in order to identify the later phases that are observed after the direct S wave during nearby intermediate-depth earthquake. Finally, the identified later phases are simulated by 2D finite-difference method.

GEOLOGICAL SETTINGS AND DATA

The Ishikari plain is located in the mid part of Hokkaido. The plain is approximately 72 km long and 34 km wide and is filled with Neogene and Quaternary sediments and formed a sedimentary basin bounded on the southwest by Sapporo Seinan mountains (Southwestern Sapporo mountains) and on the east by Hidaka mountains (Fig. 1). Sapporo Seinan mountains are primarily composed of Neogene volcanic rocks. In the study area, the sediments in the plain thicken to the center of the basin, where reach a depth of about 3 km and are underlain by early Miocene bedrock (Fig. 2). Shear-wave velocities in the sediments increase with depth from 200 m/s in the surface sediments to 3000 m/s in the bedrock (Sasatani et al., 2001).

Seismographs were deployed at 3 sites in the study area, forming a linear array running from the base of the mountain for a distance of 3 km cross the edge of the basin, as shown in Fig. 1. Note that the station TUN is just outside the Ishikari plain, while the stations KNN and MED are within. The northeast station MED forms a vertical array. This array consists of the surface and 500-m-depth seismometers. The accelerograms recorded at TUN and MED stations were integrated into ground velocities. At KNN station, a velocity seismometer (VSE-11/12) was installed.

Many earthquakes were recorded on the array between 1997 and 2004, and an earthquake was selected for use in this study (Table 1). Three components of velocity or acceleration were recorded at each station. The horizontal components (north and east) were subsequently rotated by 45° clockwise into edge-normal (EN) and edge-parallel (EP) components, while the vertical component (UD) was left unaltered.

The chosen event was intermediate depth (222 km), nearly vertically incident angle (Epicentral distance / Depth < 1) and moderate magnitudes (M 5.9). Maximum velocities of the event at the stations are less than 1 cm/s, thus nonlinearity of the soils is ignorable.

Although the incoming wavefield came from the earthquake is considered as incident vertically, a record section of the waveforms of the nearby intermediate earthquake demonstrate that later waves following S wave plays an important role in the ground-motion amplitudes for basin sites on the Ishikari plain. Figure 3 shows the record section of velocity seismograms of 2003 Feb. 19 earthquake. The record section starts with stations on rock southwest of the Ishikari plain (TUN). KNN and MED are the stations located on the sedimentary basin. There is a clear delay of about 1 s for the S wave arrival at KNN and MED compared with that at the rock site TUN, although TUN is farthest from the epicenter between 3 stations. This delay is caused by the sediments in the Ishikari plain. The velocity waveforms obtained from the stations within the Ishikari plain (KNN and MED) show large later phases arriving in the few seconds after the S waves. These basin sites also exhibit longer durations of compared with the rock site (TUN). In particular, station MED shows a distinct arrival (labeled “X” in Fig. 3) starting about 10 seconds after the S wave on the vertical components.

Table 1 The event used in this study.

Date	Epicentral distance	Station-to-epicenter azimuth	Depth	M
19 Feb 2003	118 km	N23°E	222 km	5.9

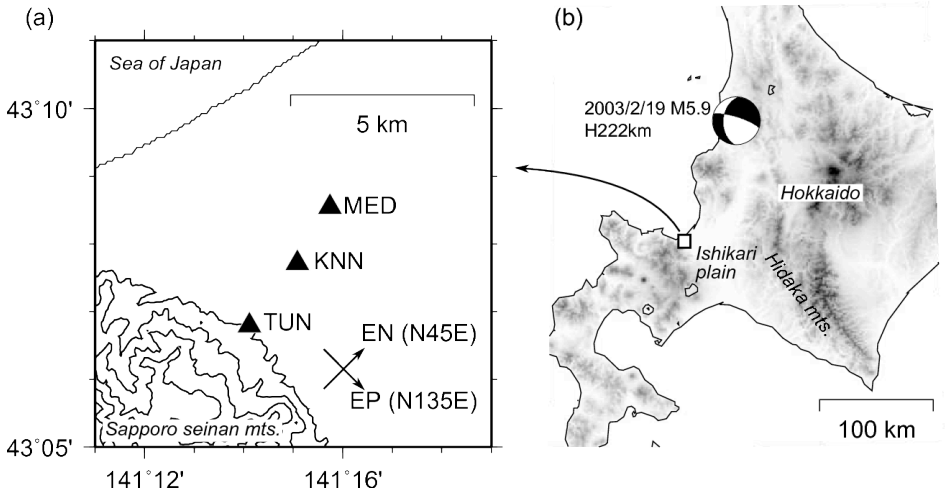

Fig. 1 (a) Map of the northwestern part of Ishikari plain showing the location of the seismic stations used in this study. EN; Edge Normal and EP; Edge Parallel. (b) Hypocentral location of the event used in this study.

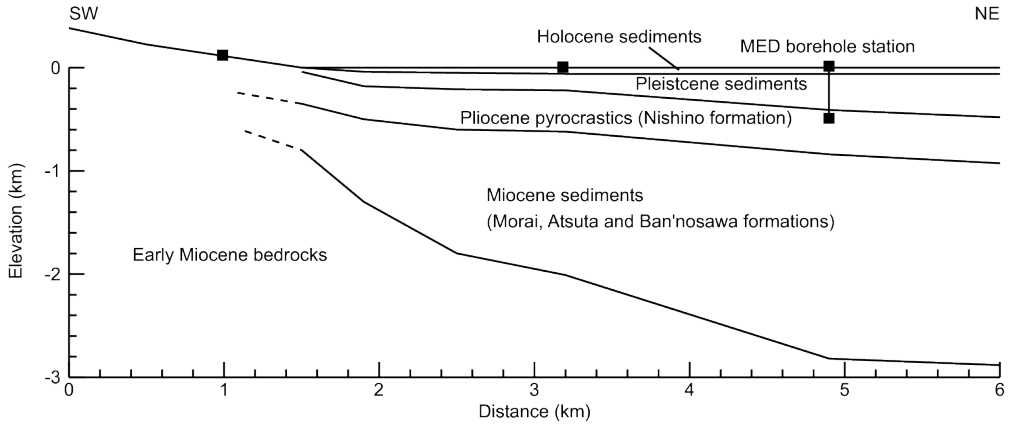

Fig. 2 Geological cross section of the northwestern part of the Ishikari plain, along the line shown in Fig. 1 (after Yoshida, 2004).

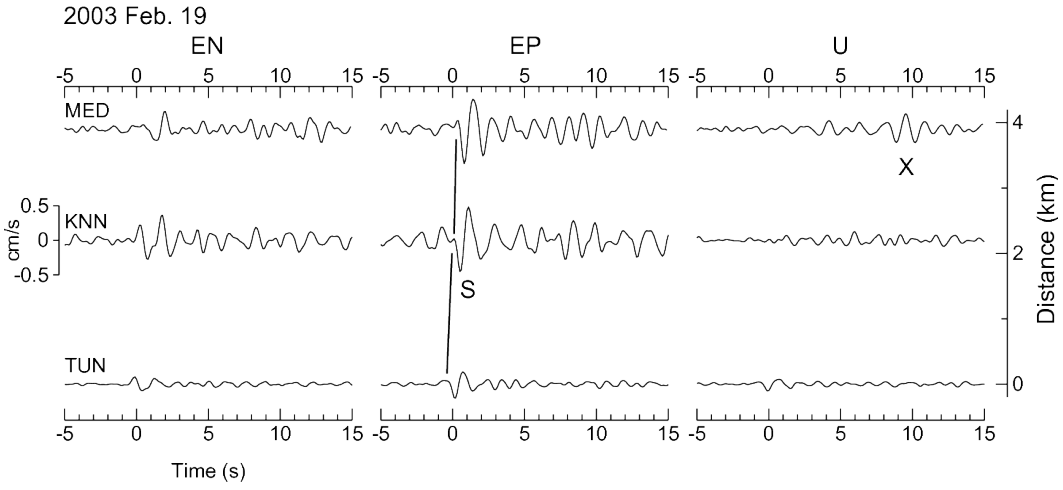

Fig. 3 Record sections of velocity waveforms for the intermediate depth earthquake (M5.9). Bandpass-filtered velocity waveforms of S wave recorded at the linear array stations. Pass-bands are 0.5-2.0 Hz. The vertical scale is distance from TUN, and the horizontal scale is time after S-wave arrival at MED. A prominent later phase (X) is indicated. EN: edge normal; EP: edge parallel; U: Up-down.

PHASE DECOMPOSITION METHOD FOR SINGLE SURFACE WAVE TYPE

In order to investigate the X phase recorded from the MED site, a vertical array analysis method for a pair of records is developed. The basic approach is similar to the method proposed by Yoshida and Sasatani (2008). Let us suppose a vertically incident plane S wave and laterally incident surface waves on a vertical array of *N* seismometers in a laterally homogeneous medium (Fig. 4). In this case, horizontal-component array seismograms consist of S, Love and Rayleigh waves. I assume that one of horizontal components consist of S wave and one kind of surface (Love or Rayleigh) wave on each of the horizontal components of a vertical array of *N* seismometers in a laterally homogeneous medium (Fig. 4). This assumption may be reasonable for analyzing response to vertically incident plain wave of a 2-D sedimentary basin, such as this study.

All time histories (u_i ; $i = 1 \cdots N$) of a horizontal component are obtained at *N* sensor points. In the time domain, time histories of ground motion at the surface ($z = z_1 = 0$) are given by

$$u_1(t) = \int_{-\infty}^{\infty} \left[\hat{S}(\omega) + \hat{F}(\omega) \right] e^{i\omega t} d\omega \tag{1}$$

for a horizontal component. Here, $\hat{S}(\omega)$, and $\hat{F}(\omega)$ are Fourier transforms of S and surface waves, respectively, at the surface. *t* is time and ω is the angular frequency.

The time histories of ground motion at the depth $z = z_i$ are given by the following equation:

$$u_i(t) = \int_{-\infty}^{\infty} \left[a_{i1} \hat{S}(\omega) + a_{i2} \hat{F}(\omega) \right] e^{-i\omega t} d\omega \tag{2}$$

where a_{i1} and a_{i2} are the transfer functions between the surface and the depth z_i for the S wave and the surface wave, respectively. By setting $a_{1j} = 1$ for the transfer functions of the surface records, I can then rewrite equations (1) in the same linear form as equations (2).

For plane waves in a 1-D layered medium, time histories of phase *j* at a certain depth can be expressed as a convolution of the time histories at the surface with a transfer function between the surface and the specified depth. The transfer function for phase *j* between the specified depth ($z = z_i$) and the surface ($z = 0$) can be defined as a simple spectral ratio $a_{ij}(\omega)$ in the frequency domain. Although the transfer functions for S wave have real and imaginary parts, those for Love and Rayleigh waves have only real values because these waves are in phase with depth. I use the surface terms as the basis of the transfer functions in this paper; this is opposite to the conventional borehole spectral ratio.

In the frequency domain, equations (1) and (2) can be rewrite in the frequency domain as

$$\hat{u}_i = a_{i1} \hat{S}(\omega) + a_{i2} \hat{F}(\omega). \tag{3}$$

I can summarize equation (3) for various depths in matrix forms at each frequency as

$$\mathbf{u} = \mathbf{A}\mathbf{x} \tag{4}$$

where, $\mathbf{u} = \begin{pmatrix} \hat{u}_1 \\ \hat{u}_2 \\ \vdots \\ \hat{u}_N \end{pmatrix}$ (array data vector), $\mathbf{A} = \begin{pmatrix} a_{11} & a_{12} \\ a_{21} & a_{22} \\ \vdots & \vdots \\ a_{N1} & a_{N2} \end{pmatrix}$ (transfer function matrix), and $\mathbf{x} = \begin{pmatrix} \hat{S} \\ \hat{F} \end{pmatrix}$ (wave model vector).

The transfer functions are obtained by the Haskell's matrix method assuming a 1-D velocity structure model. The velocity structure is

estimated by some exploration, for example, PS-logging.

From the element number of the wave model vectors, at least two time histories obtained at different depths are required for estimation. If the data obtained from two different depth seismometers, the wave model vector $\mathbf{x}$ is taken with calculating $\mathbf{A}^{-1}$. If the data obtained from the vertical array consist of more than two seismometers, the wave model vectors are estimated using the weighted least-squares method. After the wave model vectors are estimated for necessary frequencies, from 0 Hz to the Nyquist frequency, waveforms for the decomposed phases are obtained by inverse Fourier transform of the elements of the wave model vectors.

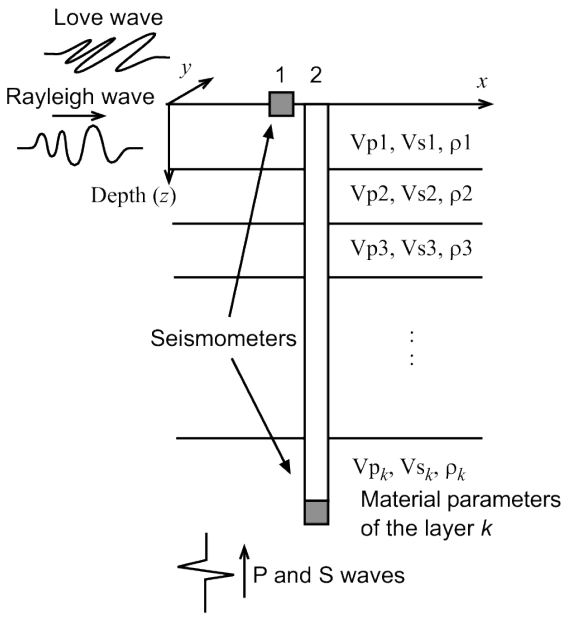

Fig. 4 Schematic diagram of a vertical array seismic observation.

SECONDARY GENERATED SURFACE WAVES IN THE ISHIKARI PLAIN

I applied the proposed method to the vertical array data obtained at MED. The gravity anomalies in the study area (Komazawa et al., 1998) suggested that the depth of the sediments increases to the northeast and that the lateral variations in NW-SE (EP) direction of the structure are small in the study area. Thus, I analyzed that surface waves in the EN and EP components are assumed to be Rayleigh and Love waves, respectively.

The transfer functions between the surface and the sensor depth were calculated by the propagator matrix method (Aki and Richards, 2002) for body waves and the compound matrix method (Saito, 1988, 1989; Saito and Kabasawa, 1993) for surface waves based on the one-dimensional velocity structure model at MED (Fig. 5). The P- and S-wave velocity structures at MED were investigated by using the PS logging (Fig. 5) and microtremor survey method (SPAC method, e.g., Okada, 2003) (Sasatani et al., 2001). Q (quality factor) values were assumed as $Q_S = V_S / 15$. Figure 6 shows the transfer functions for P, S, Love and Rayleigh waves between depths of the surface and borehole sensors. As noted in the previous section, the transfer functions for Love and Rayleigh waves have only a real part, whereas those for P and S waves have real and imaginary parts because they propagate vertically.

Observed array records of the 2003 Feb. 19 nearby intermediate-depth earthquake are analyzed assuming that Rayleigh waves are on the edge-normal component and that Love waves are on the edge-parallel component. This event had the small epicentral distance (118 km) compared to an intermediate depth of 222 km. It is thus reasonable to assume the vertical incidence of body waves to the bedrock of the plain. Prior to the decomposition, the observed records were band-pass filtered in order to avoid the instability at the low frequency; the pass band was 0.5–1.4 Hz. Then, I obtained velocity time histories by integration from the accelerograms.

Figure 7(a) shows the array velocity seismograms. A direct S wave is found at around 10 s on the EN and EP components of the velocity seismograms, although it is not found on the UD component of the velocity seismograms. This is evidence of the vertical incidence of the direct S wave at MED. There are prominent later phases following the S-wave arrival in the surface records; however, they are not so clear in the borehole records.

The array analysis results (Fig. 7b) show that the duration of the direct S wave was a few seconds and that small S waves (the S coda) follow the direct S-wave arrival. The amplitude of the decomposed surface waves at the direct S-wave arrival time was very small. The decomposed surface waves appeared about 5 s after the direct S-wave arrival, and the amplitude levels in the horizontal components were maintained for more than 30 s. The later waves identified as surface waves seemed to be basin-induced surface waves generated at the edge of the basin, because of the near and deep event. The wave packet around 21 s in the UD component (X phase in Fig. 3) was also identified as a surface wave.

The wave packet of the X phase in the decomposed surface wave shows an elliptic particle motion on the EN–UD plane (Fig. 8), which indicates a Rayleigh wave with an apparent period of 1.7 s (0.6 Hz). The theoretical amplitude ratio of the horizontal-to-vertical component of the fundamental mode Rayleigh wave calculated from the velocity structure at MED (Fig. 5) is about 1 (prograde motion), for the period of 1.7 s. It suggests that this wave packet is Rayleigh wave propagating from southwest to northeast.

The delay time of the wave packet of the X phase from the S wave (about 9 seconds) and a group velocity of the fundamental-mode Rayleigh wave suggests that this wave packet was originated from the southwestern basin edge located at about 3 km southwest of the MED station. The group velocity calculated from the velocity structure at MED is about 0.34 km/s at the period of 1.7 s. Distance from the origin of the wave packet is estimated to be about 3 km (= 9 x 0.34), which is calculated from the delay time (9 s) and the group velocity (0.34 km/s). The wave packet seems to be a basin-induced surface wave (Kawase, 1996) excited at the basin edge.

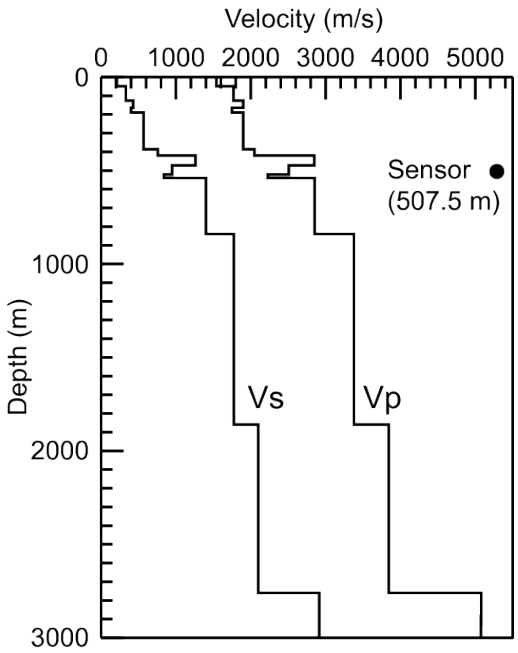

Fig. 5 Array layout and subsurface velocity structure of the MED vertical array.

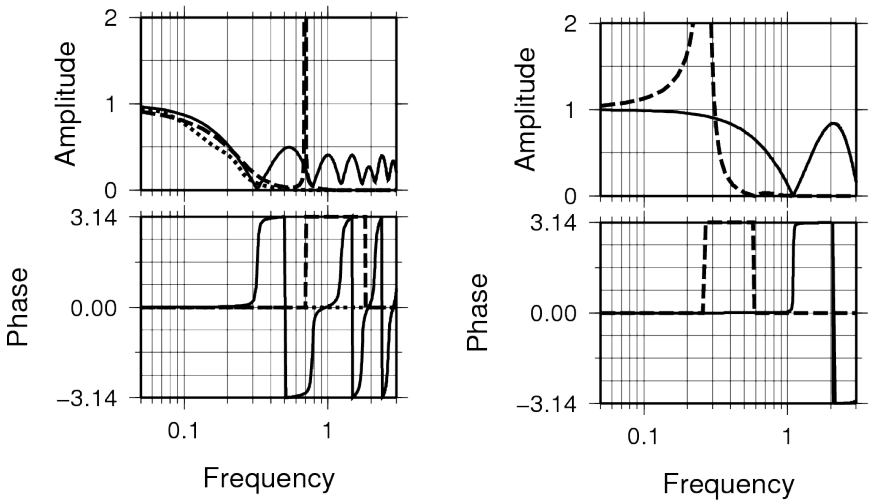

Fig. 6 Spectral ratios (transfer functions) for various seismic phases. The spectral ratio is obtained by dividing a phase at a certain depth by the phase at the surface. The upper panel shows the amplitude ratios, and the lower panel shows the phase differences. Solid, dotted, and dashed lines indicate body (P and S), Love, and Rayleigh waves, respectively. Negative values of the transfer functions of Rayleigh waves are shown as a phase shift of π. Note that the numerator and denominator are opposite to those of a conventional borehole spectral ratio.

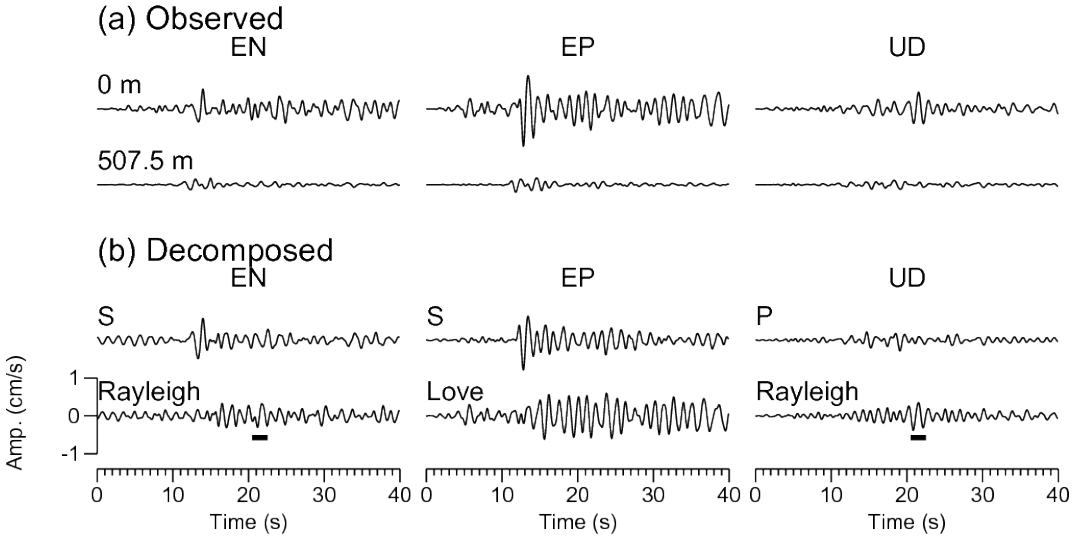

Fig. 7 (a) Vertical array records at MED for a nearby intermediate-depth earthquake. These are band-pass filtered velocity seismograms: the pass band is from 0.5 to 1.4 Hz. (b) Vertical array analysis results: the decomposed waveforms.

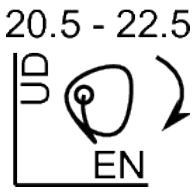

Fig. 8 The particle motion of the decomposed surface waves in the EN–UD plane. The time window for the particle motion is shown by the solid line under the waveforms in Fig. 7b. A curved arrow indicates the mode of elliptic motion.

2-D FD SIMULATION OF LATER PHASES

I have used 2-D finite-difference ground-motion simulations to confirm that the identified surface waves by the phase decomposition analysis are generated by the effect of the sedimentary basin structure. A 2-D model for P- and S-wave velocities and density (Fig. 9) was constructed for the northwestern part of the Ishikari plain from borehole loggings, microtremor array surveys, seismic reflection data, and Bouguer anomaly data (Yoshida, 2004). The cross section approximately follows the line of linearly deployed instruments. Model of boundary depths of the Holocene and Pleistocene layers, whose depth reaches to more than 400 m, are mainly determined from logging data. Microtremor array surveys, seismic reflection data, and Bouguer anomaly data are used to determine deep velocity structures (e.g., Sasatani et al., 2001). P- and S-wave velocities have gradients in most of layers, since borehole PS-logging profiles exhibit gradients (Yoshida and Sasatani, 2000).

Responses from the 2-D model to vertically incident plane SV and SH waves are simulated. The simulation is divided into in-plane (P-SV) and anti-plane (SH) problems. Time steps of 0.00125 s (P-SV) and 0.002 s (SH) were used. Incident waveforms are a Herrmann's pulse (Herrmann, 1979) width 0.75 s. The model is discretized at 10-m grid spacing. I use the absorbing boundary conditions of Clayton and Engquist (1977), and the sides of the computational model are padded with homogeneous regions of attenuative material to further limit reflections from the boundaries of the grid (Cerjan et al., 1985).

Figure 10 compares the observed velocity seismograms for the event to the synthetics calculated by a 2-D finite difference method for a sedimentary basin model assuming vertical incident plain SH and SV waves. Following Wen and Helmberger (1997), I use the station TUN as the reference station and calculated the transfer functions of the basin stations relative to it from the results of the finite-difference simulation, then predict the synthetics of the stations inside the basin (KNN and MED) by convoluting the recording at the station TUN with the transfer function. The observed records are good agreement with synthetic seismograms in the maximum amplitudes and general waveforms of significant wave trains at most sites. For example, the synthetic reproduces the later phase arrived about 10 s after the initial S wave (X phases) at station MED.

Although the general agreement between synthetics and observations is good at most stations, the synthetics tend to somewhat overpredict the amplitude of the records. It is suggested that the omission of anelastic attenuation causes this discrepancy.

The record sections of the simulation results (Figs. 11 and 12) show significant later phases following the direct S wave inside the basin. Although the waveforms at TUN site (10 km) are very simple, duration of the waveforms inside the basin are very long. Figure 11 shows that the later phases whose horizontal and vertical motions are out of phase by 90° propagate with a group velocity of 0.35–0.40 km/s into right side (the direction for the basin center). Figure 12 also shows that the later phases following the S wave propagate with the group velocity of about 0.25 km/s. These result shows that the later phases are basin-induced surface waves excited at the basin edge around 10.8 km.

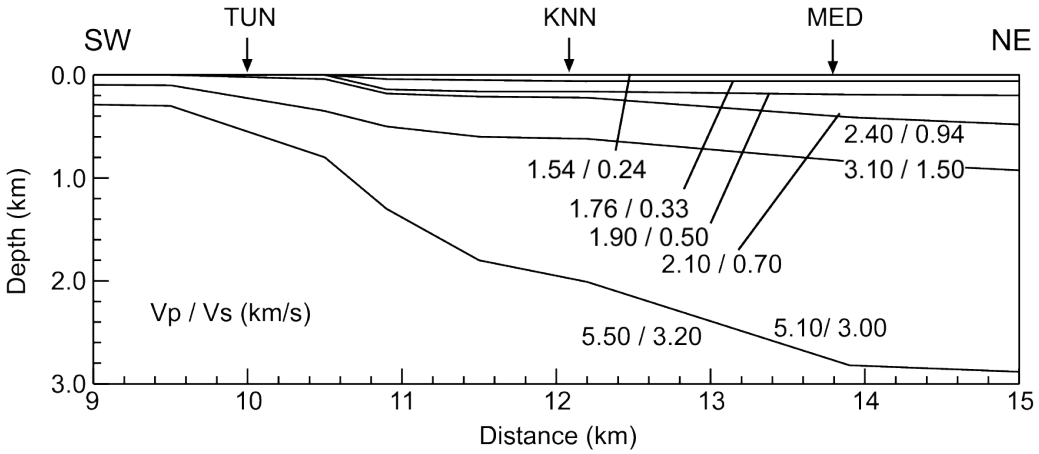

Fig. 9 Velocity structure model used in the 2-D finite-difference simulation. Locations of the stations are indicated above the model.

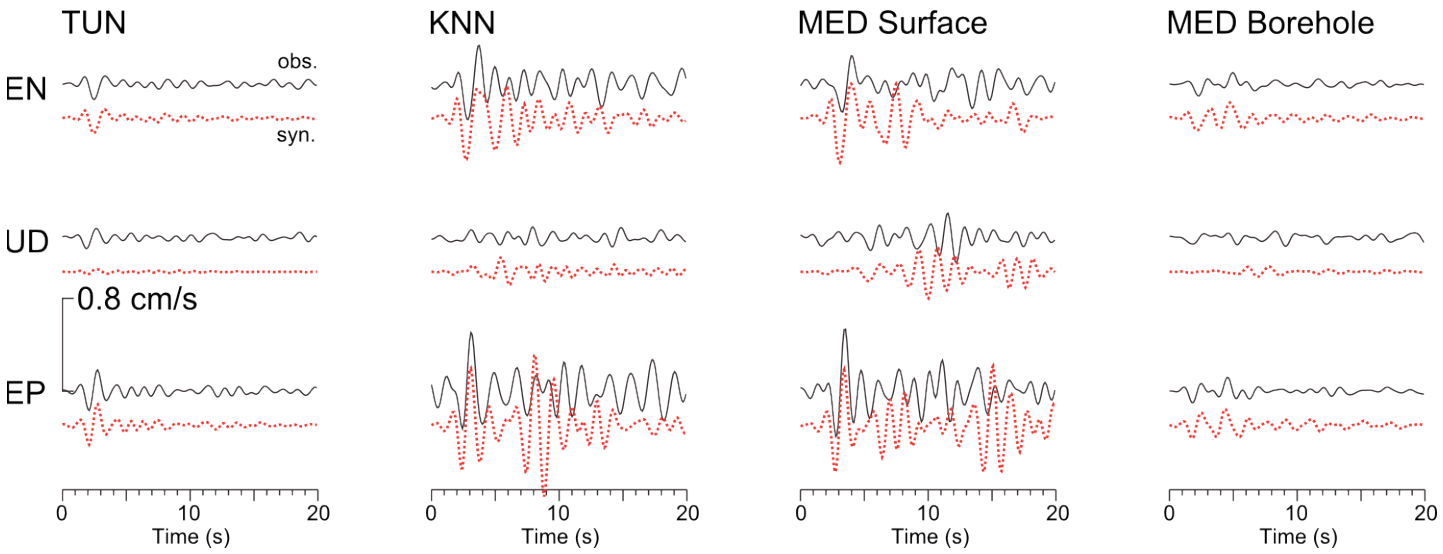

Fig. 10 Comparison of the 2003 Feb. 19 Rumoi M_{JMA} = 5.9 earthquake data (solid black lines) and the synthetic seismograms (dotted red lines). Records of KNN and MED are calculated by convolving the TUN record and the synthetic transfer functions calculated with 2-D finite-difference method. Note that the synthetics of TUN are identical to the observations.

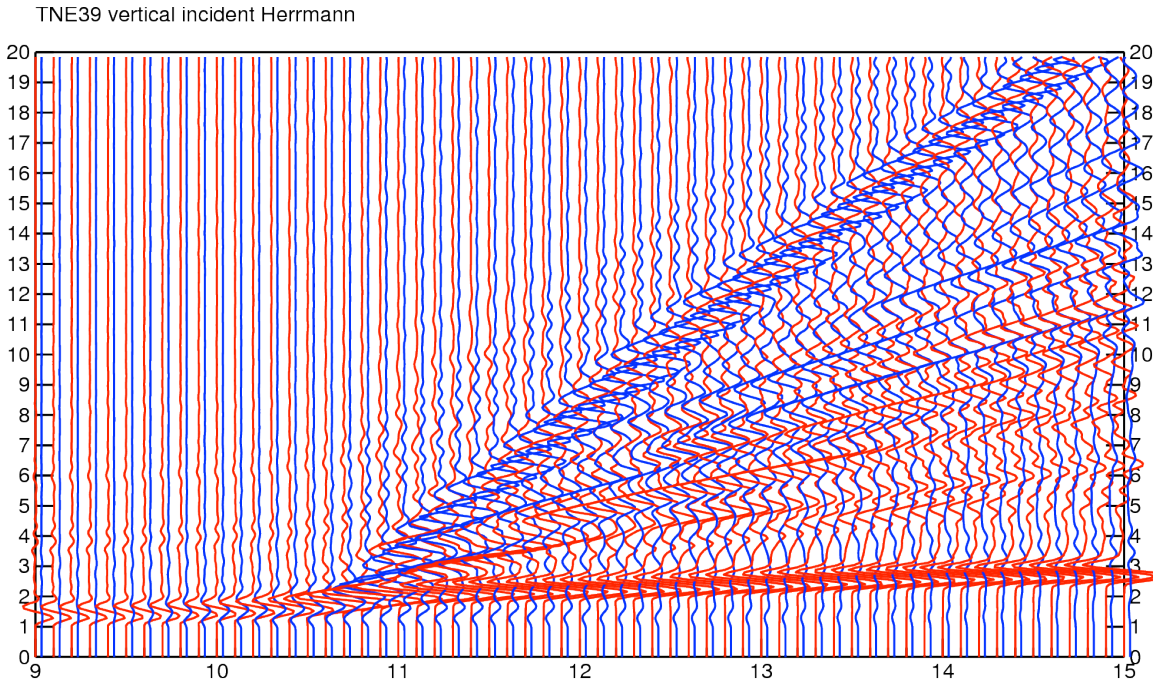

Fig. 11 Synthetic seismograms from in-plane (P-SV) 2D simulation. Blue and red lines show UD and EP components, respectively. The vertical scale is time (s) and the horizontal scale is distance (km), which is corresponding to that of Fig. 9.

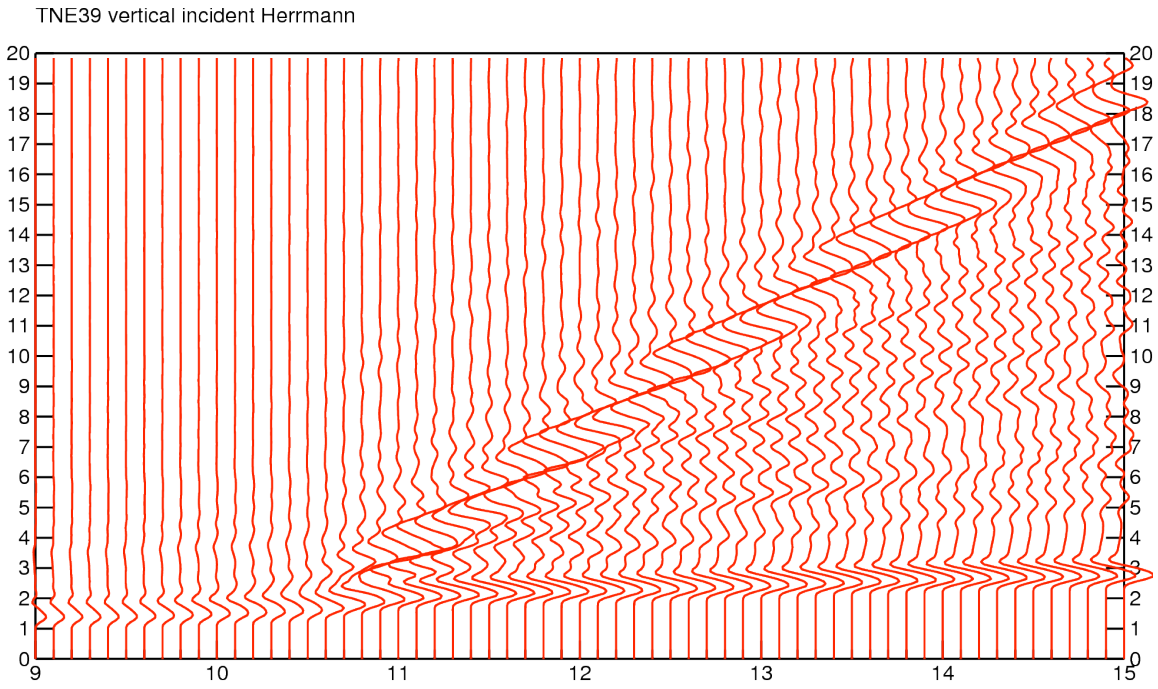

Fig. 12 Synthetic seismograms from anti-plane (SH) 2D simulation. The vertical scale is time (s) and the horizontal scale is distance (km), which is corresponding to that of Fig. 9.

CONCLUSION

Significant later phases following the direct S wave on the record from the nearby intermediate depth earthquake are observed at the basin stations on the Ishikari plain. In order to investigate these later phases, the vertical array analysis method (Yoshida and Sasatani, 2008) was modified for decomposing vertical array records into S and surface waves. The modified phase decomposition method is successfully applied for the vertical array data from the nearby intermediate earthquake. The observed later phases are identified as surface waves by the proposed method. These surface waves were confirmed as basin induced surface waves by 2-D finite-difference simulation.

References

Aki, K. and P. G. Richards [2002], "*Quantitative Seismology*". University Science Books, Sausalito.

Cerjan, C., D. Kosloff, R. Kosloff, and M. Reshef [1985], "A nonreflecting boundary condition for discrete acoustic and elastic wave equations", *Geophysics*, vol. 50, pp. 705–708.

Clayton, R. and B. Engquist [1977], "Absorbing Boundary Conditions for Acoustic and Elastic Wave Equations", *Bull. Seism. Soc. Am.*, vol. 67, pp. 1529–1540.

Fletcher, J. B. and K.-L. Wen [2005], "Strong Ground Motion in the Taipei Basin from the 1999 Chi-Chi, Taiwan, Earthquake", *Bull. Seism. Soc. Am.*, vol. 95, pp. 1428–1446.

Graves, R. W. [1993], "Modeling Three-Dimensional Site Response Effects in the Marina District Basin, San Francisco, Carifornia", *Bull. Seism. Soc. Am.*, vol. 83, pp. 1042–1063.

Herrmann, R. B. [1979], "SH-Wave Generation by Dislocation Sources–A Numerical Study", *Bull. Seism. Soc. Am.*, vol. 69, pp. 1–15.

Hisada, Y., K. Aki, and T.-L. Teng. [1993], "3-D Simulations of Surface Wave Propagation in the Kanto Sedimentary Basin, Japan

Part 2: Application of the Surface Wave BEM", *Bull. Seism. Soc. Am.*, vol. 83, pp. 1700–1720.

Kawase, H. [1996], "The Cause of the Damage Belt in Kobe: "The Basin-Edge Effect," Constructive Interference of the Direct S-Wave with the Basin-Induced Diffracted/Rayleigh Waves", *Seism. Res. Lett.*, vol. 67, pp. 25–34.

Koketsu, K., K. Hatayama, T. Furumura, Y. Ikegami, and S. Akiyhama [2005], "Damaging Long-period Ground Motions from the 2003 Mw8.3 Tokachi-oki, Japan Earthquake", *Seism. Res. Lett.*, vol. 76, pp. 67–73.

Komazawa, M., T. Hiroshima, Y. Murata, M. Makino, and R. Morijiri [1998]. "*Gravity Map of Sapporo District (Bouger Anomalies)*". Geological Survey of Japan.

Okada, H. [2003]. "*The microtremor survey method*". geophysical monograph series, no. 12. Society of Exploration Geophysicists.

Olsen, K. B. and R. J. Archuleta [1996], "Three-Dimensional Simulation of Earthquakes on the Los Angeles Fault System", *Bull. Seism. Soc. Am.*, vol. 86, pp. 575–596.

Ozel, O. and T. Sasatani [2004], "A Site Effect Study of the Adapazri Basin, Turkey, from Strong and Weak-Motion Data", *Journal of Seismology*, vol. 8, pp. 559–572.

Saito, M. [1988], "DISPER80: A Subroutine Package for the Calculation of Seismic Normal-Mode Solutions". in Doornbos, D. J., editor, "*Seismological Algorithms*", pp. 293–319. Academic Press, San Diego.

Saito, M. [1989], "Computations of Reflectivity and Surface Wave Dispersion Curves for Layered Media I. Sound Wave and SH Wave", *Butsuri-tanko*, vol. 32, pp. 15–26. (in Japanese with English abst.).

Saito, M. and H. Kabasawa [1993], "Computations of Reflectivity and Surface Wave Dispersion Curves for Layered Media II. Rayleigh Wave Calculations", *Butsuri-tansa*, vol. 46, pp. 283–298. (in Japanese with English abst.).

Sasatani, T., K. Yoshida, H. Okada, O. Nakano, T. Kobayashi, and S. Ling [2001], "Estimation of Deep Subsurface Structures and Observation of Strong Ground Motions in Sapporo Urban Districts", *Journal of Japan Society for Natural Disaster Science*, vol. 20, pp. 325–342.

Uetake, T. and K. Kudo [1998]. "The Excitation of Later Arrivals in Ashigara Valley during Earthquakes Occurring in East Part of Yamanashi Prefecture". in "*Proc. of the second intl. symposium on the Effects of Surface Geology on Seismic Motion"*, pp. 427–434. Balkema, Rotterdam.

Wen, L. and D. V. Helmberger [1997], "Propagational corrections for basin structure: Landers earthquake", *Bull. Seism. Soc. Am.*, vol. 87, pp. 782–787.

Yoshida, K. [2004]. "*A Study of the Seismic Response of a Sedimentary Basin – The Northern Part of the Ishikari Plain, Japan–*". PhD thesis, Hokkaido University.

Yoshida, K. and T. Sasatani [2000], "Seismic Response of Sedimentary Layers in Sapporo Derived from Borehole Seismometer Array", *Geophys. Bull. Hokkaido Univ.*, no. 63, pp. 43–64.

Yoshida, K. and T. Sasatani [2005], "Long-period Ground Motion in the Northwestern Part of the Ishikari Plain during the 2003 Tokachi-oki Earthquake", *Zisin 2*, vol. 58, pp. 107–113.

Yoshida, K. and T. Sasatani [2006]. "A Seismic Phase Decomposition Method Using Vertical Array Records". in *Third International Symposium on the Effects of Surface Geology on Seismic Motion*, pp. 175–184.

Yoshida, K. and T. Sasatani. [2008], "Seismic vertical array analysis for phase decomposition", *Geophys. Jour. Inter.*, vol. 174, pp. 707–718.